2372
doi:10.1017/S1431927622009102
Microsc. Microanal. 28 (Suppl 1), 2022

Application of a Novel Electron Energy Filter Combined with a Hybrid-Pixel Direct Electron Detector for the Analysis of Functional Oxides by STEM/EELS with Focus on Weak Signals and High Spatio-Temporal Resolution

Rolf Erni[1*], Alicia Ruiz Caridad[1], Alexander Vogel[1] and Marta D. Rossell[1]

[1.] Electron Microscopy Center, Empa – Swiss Federal Laboratories for Materials Science and Technology, Dubendorf, Switzerland.
* Corresponding author: rolf.erni@empa.ch

Numerous dedicated, highly sensitive analytical methods are in use, which reliably provide quantitative information on trace elements, dopant concentrations or impurities on the micron scale. The challenge in electron microscopy is to translate this high analytical sensitivity to small scales, namely to the nanometer or even to the atomic length scale, where similar information is required to understand the functionality of nanomaterials. The actual challenge is twofold amplified, namely by the fact that an electron transparent sample provides merely a tiny volume of matter, where elements at small concentrations are sparse in number. Secondly, the electron dose needs to be small enough to warrant the integrity of that tiny volume of matter, which might otherwise damage under electron irradiation. In order to address these challenges, various technological breakthroughs have been realized in the past decades, which, for instance, led to the detection of individual atoms by electron energy-loss spectroscopy (EELS) [1] and energy dispersive X-ray spectroscopy [2]. More recently, advanced detectors have been implemented in electron energy-loss spectrometers, which capture practically noise-free individual electrons, and thus enable the detection of weak signals, which with conventional detection technologies would have been buried in intrinsic detector noise.

In this contribution we present data collected on a FEI Titan Themis transmission electron microscope operated at 300 kV equipped with a probe aberration corrector. This microscope was recently retrofitted with a novel post-column electron energy filter CEFID, from CEOS GmbH [3]. This filter is normally supplied with a TVIPS TemCam XF416 camera, which in its retractable version allows for installing an additional detector behind it. In our case, a hybrid-pixel ELA detector from Dectris Ltd. [4] is added. This detector is equipped with a silicon chip, which in principle is sub-optimal for the detection of 300 keV electrons. Nevertheless, we tested and explored this setup for the analysis of functional oxides, with focus on detecting small quantities of trace elements, for atomic-scale mapping of high-energy core-loss excitation edges and for high-speed acquisitions in regard of in-situ and operando measurements. As the base microscope is operated with a high-brightness field emission source, without electron monochromator, of nominal energy spread of about 0.8 eV, high-energy resolution was not a main target in the herein reported applications.

A first example that demonstrates the high sensitivity of this experimental setup is a study of Er-doped Yttrium-Stabilized Zirconia (YSZ). This material is being developed and investigated with regard to its potential use as a photonic material for optical amplification. The material consists of a nanoscale layered structure, where YSZ layers with nominally 0.5 at.% Er are alternated with YSZ layers that contain 4 at.% Er. Using the Er $M_{5,4}$ excitation edge around 1400 eV energy loss, the expected modulation of the small Er concentration can be mapped directly and reveals an Er-enriched layer thickness of less than 1 nm (Fig. 1(a,b)). The elemental data of Er can be complemented with the EELS elemental maps of Y and Zr using their $L_{3,2}$ edges around 2080 and 2220 eV energy loss, respectively.

Another application concerns La(Mn,Ni)O_3, a ferromagnetic material grown as thin film on $SrTiO_3$, where the influence of the film thickness on its order parameter was investigated. Despite the limited amount of energy channels of the ELA detector (1024), the post-slit optics of the CEFID filter, based on a quadrupole projective, allows for assessing excitation edges ranging from Sr $M_{5,4}$ to La $M_{3,2}$ edges in one energy window. The corresponding elemental maps provide direct evidence of the ordered occupation of the lattice sites of Mn and Ni (Fig. 1(c)).

In summary, our first STEM/EELS applications with the CEFID filter combined with the ELA detector focused on elemental maps and for challenging the detection of weak signals over a large energy range. The excellent optics of the energy filter allows us to work with a large entrance aperture without compromising on the energy resolution for our applications. With electron beam currents in the range of 200-500 pA, the large entrance aperture along with the high sensitivity of the ELA camera makes signal detection with acquisition times in the order of 1-5 ms feasible, even for capturing signals of elements at low concentration or with corresponding high-energy excitation edges [5].

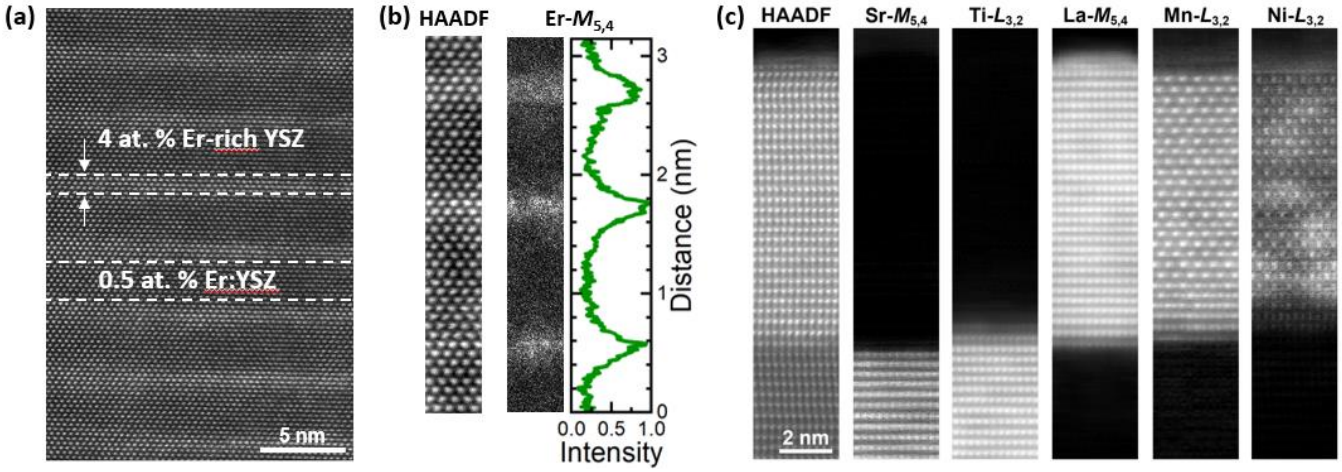

Figure 1. (a) Cross-sectional HAADF-STEM image of an Er-doped YSZ multilayer sample showing the presence of 4 and 0.5 at.% Er-containing layers. **(b)** Survey HAADF-STEM image and corresponding map of the Er-$M_{5,4}$ edge along with the normalized intensity profile extracted over the full Er map width. **(c)** Survey HAADF-STEM image of a La(Mn,Ni)O_3 film grown of $SrTiO_3$ and corresponding maps of the Sr-$M_{5,4}$, Ti-$L_{3,2}$, La-$M_{5,4}$, Mn-$L_{3,2}$, and Ni-$L_{3,2}$ edges. Note that the Ni map appears rather noisy as the Ni-$L_{3,2}$ edges strongly overlap with the intense La-M_4 line. The EELS maps in **(b)** and **(c)** have been recorded with dwell times of 5 and 1 ms, respectively, without drift correction.

References:

[1] M. Varela et al., Phys. Rev. Lett. **92** (2004), 095502. doi: 10.1103/PhysRevLett.92.095502.
[2] T. C. Lovejoy et al., Appl. Phys. Lett. **100** (2012), 154101. doi: 10.1063/1.3701598.
[3] F. Kahl et al., Adv. Imaging Electron Phys. **212** (2019), 35. doi: 10.1016/bs.aiep.2019.08.00.
[4] B. Plotkin-Swing et al., Ultramicroscopy **217** (2020), 113067. doi: 10.1016/j.ultramic.2020.113067.
[5] The authors acknowledge financial support by SNF projects 206021_189625 and 200021 175926. The LMNO sample was provided by Dr. G. De Luca and Prof. M. Gibert, TU Vienna (AT).